

# LIAISE GLORI 2021 datasets

Karin Dassas, Pascal Fanise, Michel Le Page, Emna Ayari, Philippe Baillion,  
Mateo Sige, Aaron Boone, Mehrez Zribi



- Datapaper overview
- Datapaper datasets descriptions
- Soil Moisture Estimation dataset

## Data in Brief



ELSEVIER

[Volume 52](#), February 2024, 109850



**Karin Dassas, Pascal Fanise, Michel Le Page, Emna Ayari, Philippe Baillion, Mateo Sige, Aaron Boone, Mehrez Zribi**, Polarimetric instrument Global Navigation Satellite System - Reflectometry airborne data, Data in Brief, Volume 52, 2024, 109850, <https://doi.org/10.1016/j.dib.2023.109850>.

[Volume 52](#), February 2024, 109850

Data in Brief



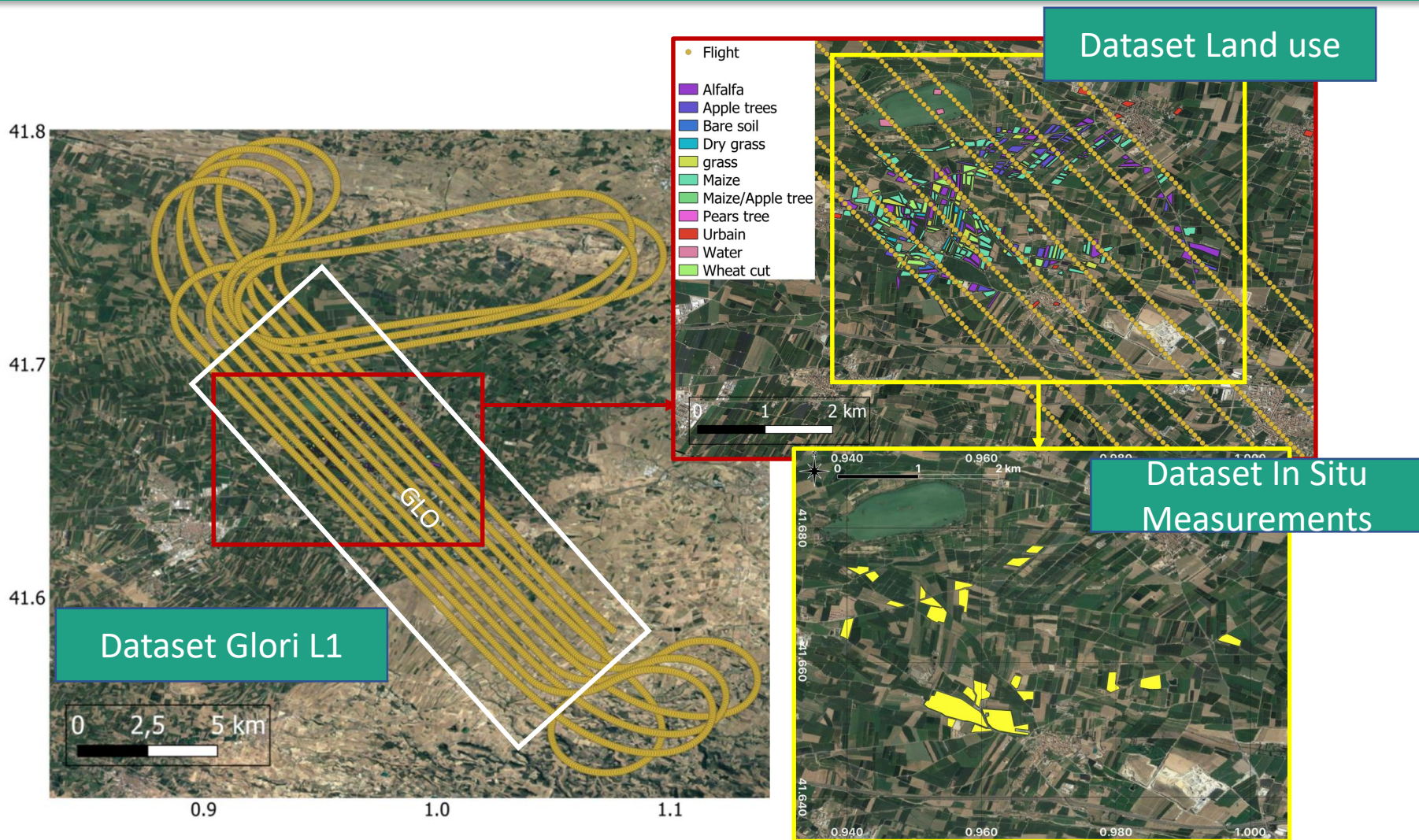
ELSEVIER

**[LIAISE GNSS-R GLORI CESBIO v1 2021 dataset: https://doi.org/10.25326/494](https://doi.org/10.25326/494)**

**[LIAISE In situ measurements CESBIO v1 dataset https://doi.org/10.25326/493](https://doi.org/10.25326/493)**

**[LIAISE Land use CESBIO v1 dataset: https://doi.org/10.25326/495](https://doi.org/10.25326/495)**

**+ [LIAISE Soil Moisture Estimation CESBIO v1. \[Dataset\]. Aeris. https://doi.org/10.25326/601 \(not in the datapaper\)](https://doi.org/10.25326/601)**

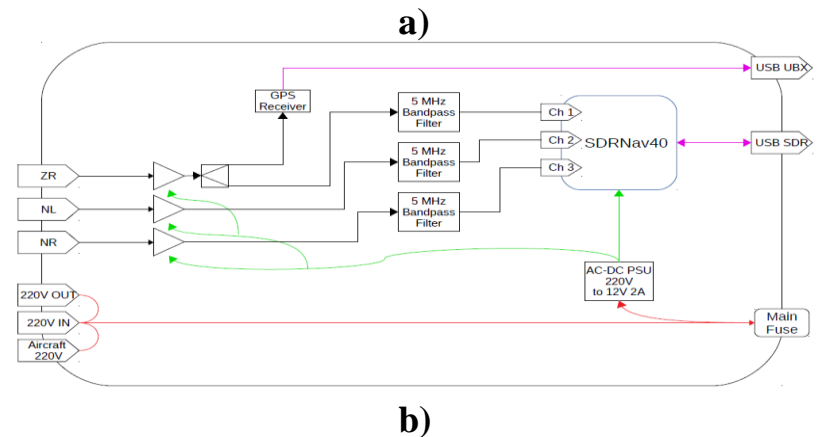
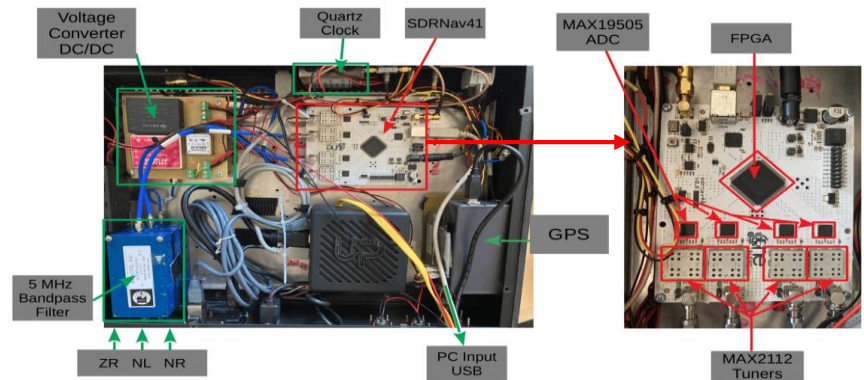
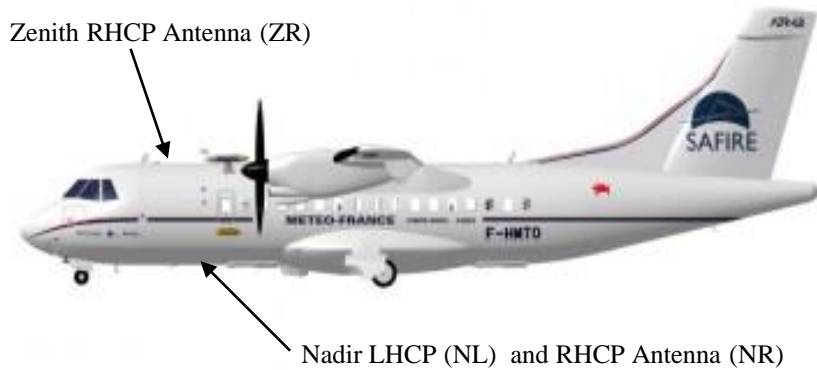


Flight path with the GLO transects zone (white frame), (left panel), land use plots (upper right image) and plots with in situ measurements (yellow plots, bottom right image)

# LIAISE GNSS-R GLORI CESBIO v1 2021 dataset

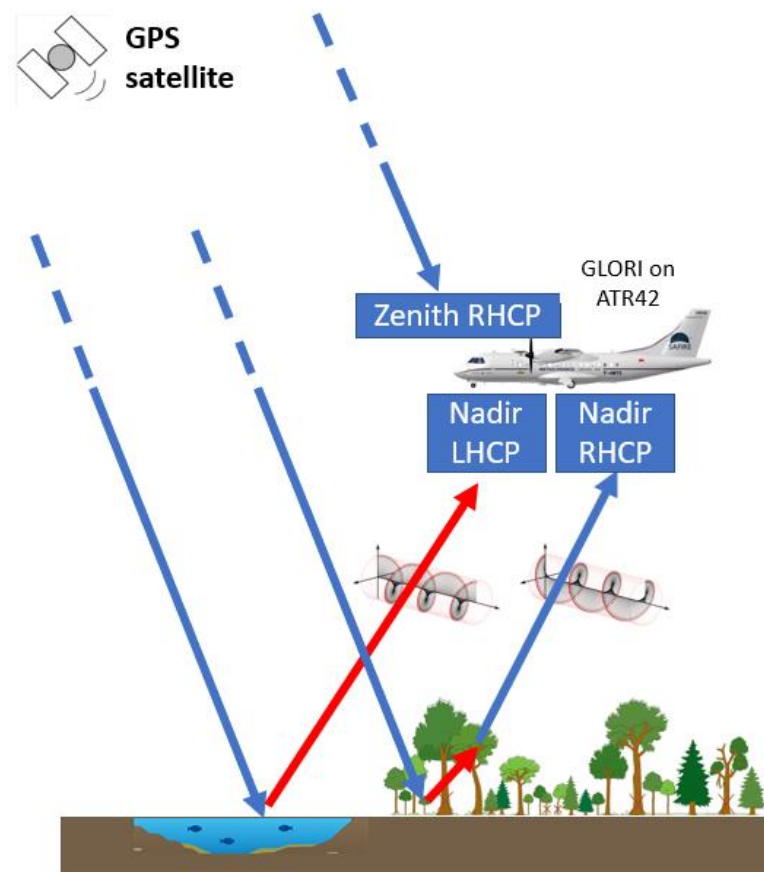
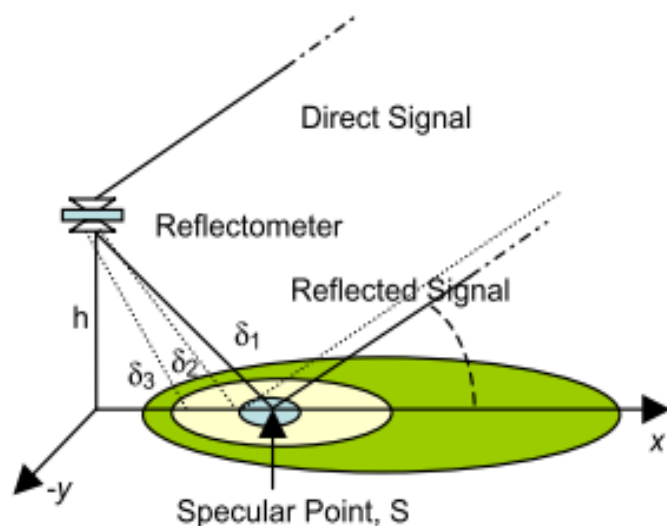


Data L1b from GLORI : **G**LObal navigation satellite system **R**eflectometry **I**nstrument



GLORI 2021 Front End (a) picture and (b) synoptic view

**GNSS REFLECTOMETRY (GNSS-R: GLOBAL NAVIGATION SATELLITE SYSTEM - REFLECTOMETRY)** is a bistatic radar remote sensing technology (transmitters and receivers are not in the same place) that uses microwave signals of opportunity from radio navigation constellations.



**GNSS-R by waveform analysis technique:** each antenna pair corresponds to a channel that measures the direct signal with its up-looking antenna and another channel measuring the signal reflected by the surface with its down-looking antenna.

J. Darrozes, N. Roussel, M. Zribi, 2016.

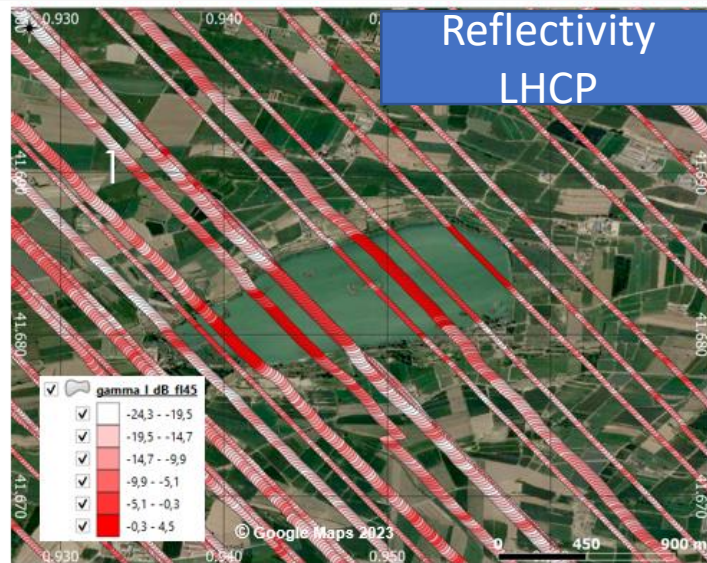


## GLORI Instrument

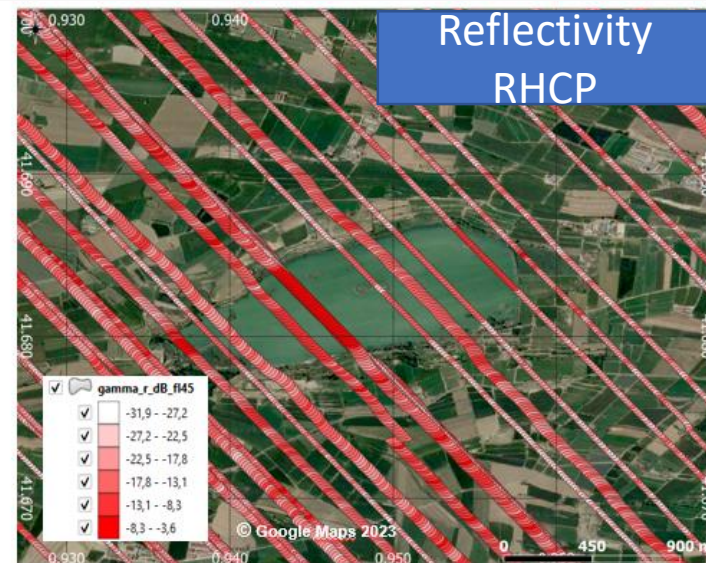
gamma_l	LHCP reflectivity ( $\Gamma_l$ from step 2 from pipeline)	float	dB
gamma_r	RHCP reflectivity ( $\Gamma_r$ from step2 from pipeline)	float	dB
noise_fix	noise fix	float	dB
noise_nl	noise floor of reflected LHCP signal	float	dB
noise_nr	noise floor of reflected RHCP signal	float	dB
noise_zr	noise floor of direct signal	float	dB
incoherent_ratio_l	incoherent ratio LHCP ( $\alpha_l$ from step 2 from pipeline)	float	n/a
incoherent_ratio_r	incoherent ratio RHCP ( $\alpha_r$ from step 2 from pipeline)	float	n/a
phase_l	LHCP phase difference relative to direct	float	Rad
phase_r	RHCP phase difference relative to direct	float	Rad
snr_nl	nadir LHCP signal to noise ratio	float	dB
snr_nr	nadir RHCP signal to noise ratio	float	dB
snr_zr	zenith RHCP signal to noise ratio	float	dB

All elevations &gt;30°

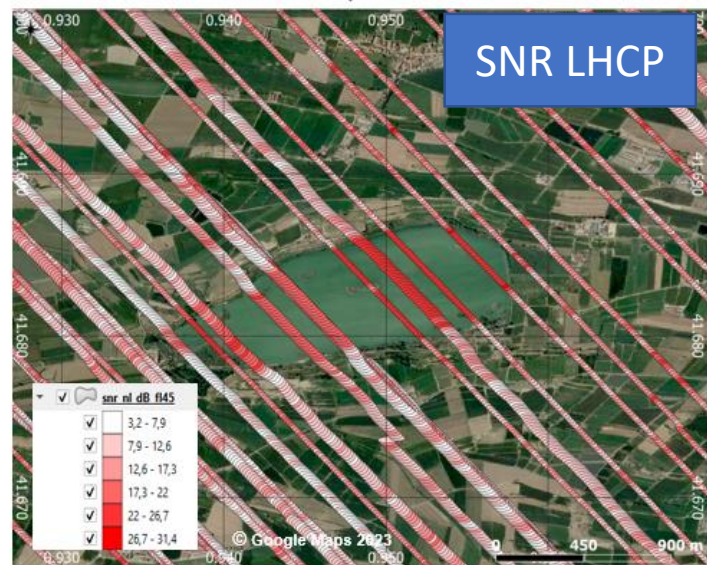
# LIAISE GNSS-R GLORI CESBIO v1 2021 dataset



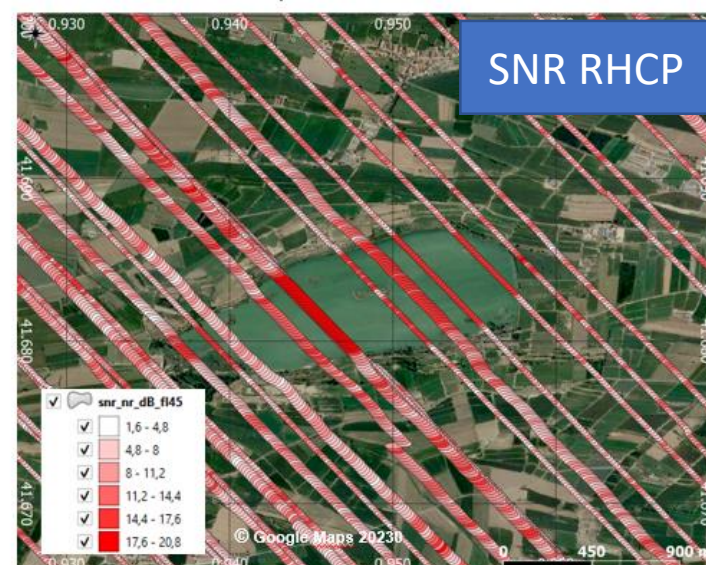
a)



b)



c)



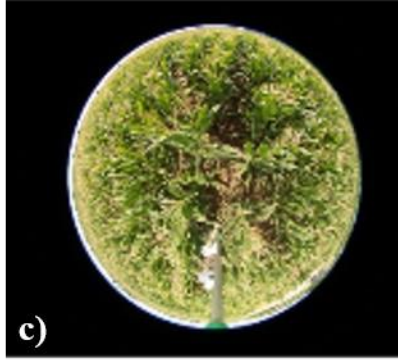
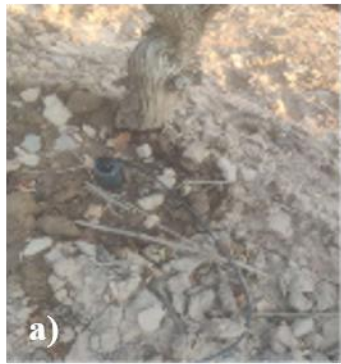
d)

(a) reflectivity left  $\Gamma_l$  (b) reflectivity right  $\Gamma_r$  and (c)  $snr_{nl}$  (d)  $snr_{nr}$  over the Ivars lake, flight 45.

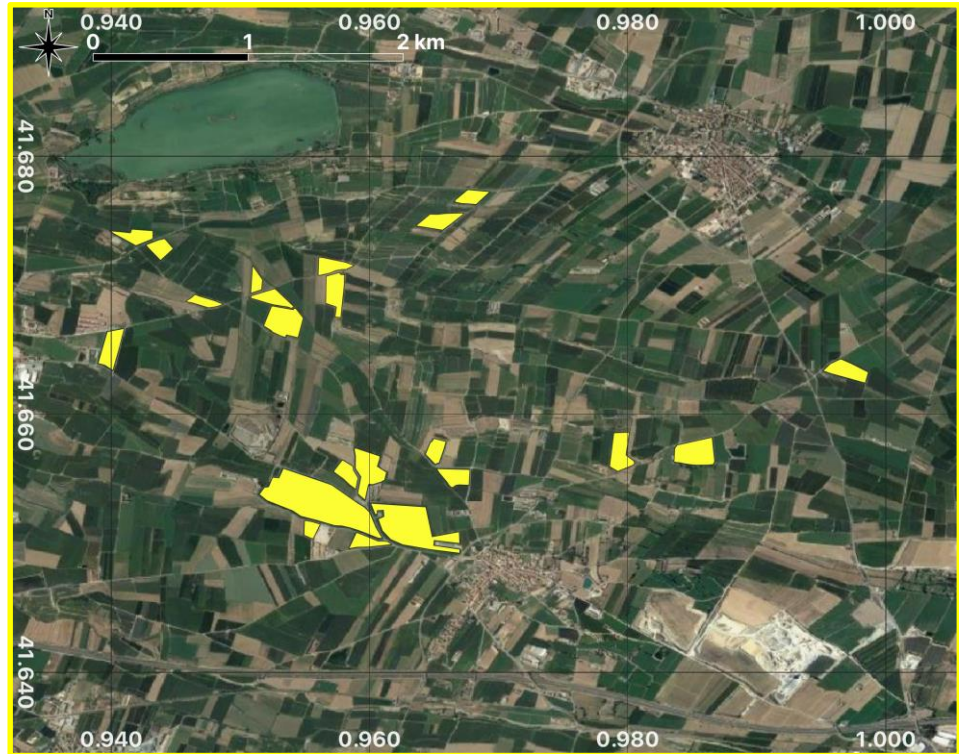
# LIAISE In situ measurements CESBIO v1 dataset



# LIAISE In situ measurements CESBIO v1 dataset



(a) soil moisture probe (b) a pin profiler picture, plot 25 (alfalfa), on July 23 (c) hemispherical photo maize.



Plots with in situ measurements

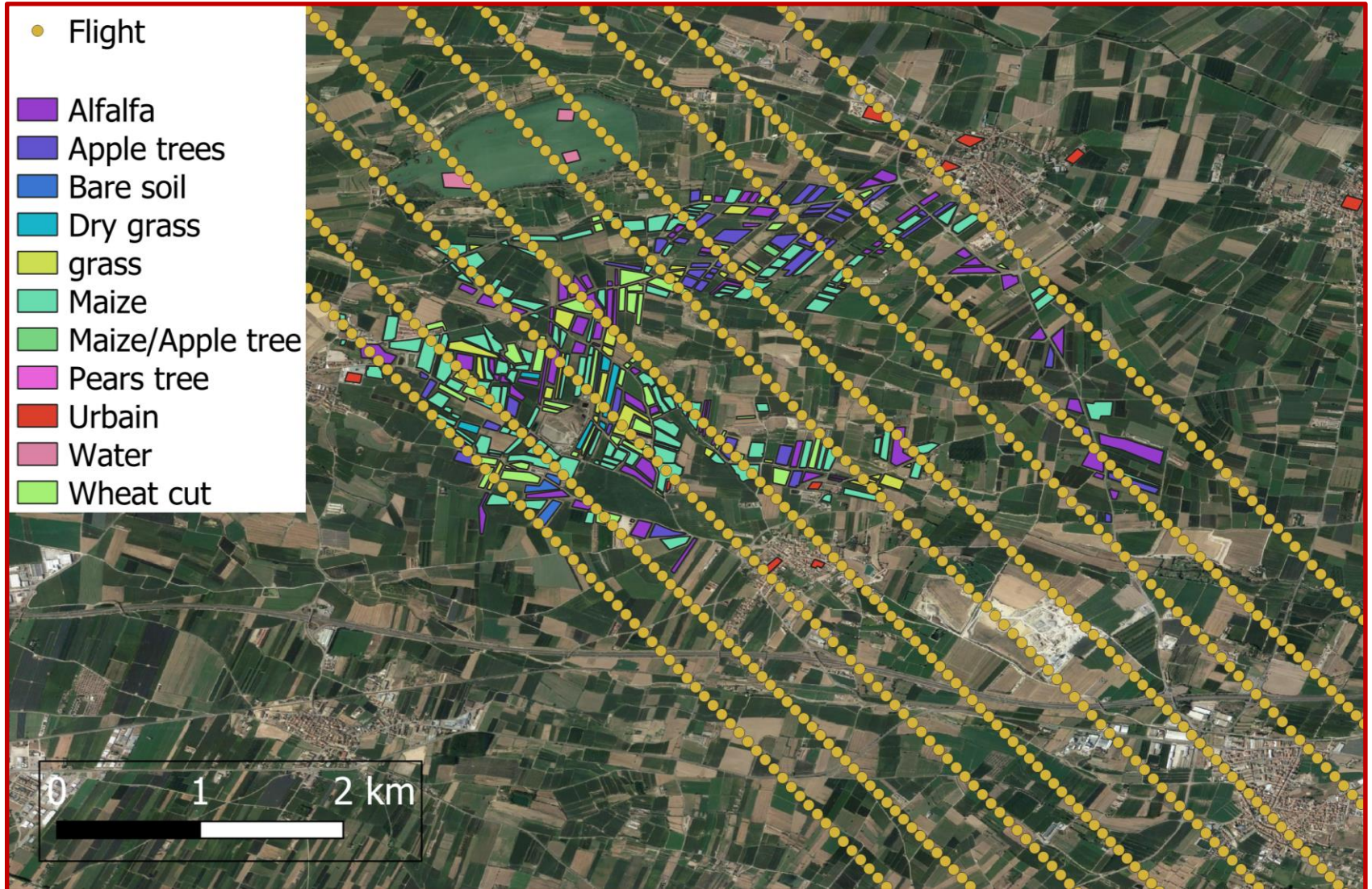
# LIAISE In situ measurements CESBIO v1 dataset

Date	HRMS (cm)	Roughness_correlation_length (cm)	$SSM_{mean}$ (m <sup>3</sup> /m <sup>3</sup> )	LAI_mean_57deg (m <sup>2</sup> /m <sup>2</sup> )
15/07/2021			[0.1-0.41]	
16/07/2021			[0.09-0.39]	
17/07/2021			[0.07-0.46]	
19/07/2021				[1.07-2.54]
20/07/2021			[0.02-0.41]	
21/07/2021			[0.04-0.38]	
<b>22/07/2021</b>			[0.06-0.34]	
23/07/2021	[0.4-1.84]	[4.112.18]		[0-3.14]
<b>27/07/2021</b>	-	-	[0.12-0.41]	-
<b>28/07/2021</b>	-	-	[0.1-0.44]	
29/07/2021				[0.15-3.42]

Contact : M. Le Page / M.Zribi

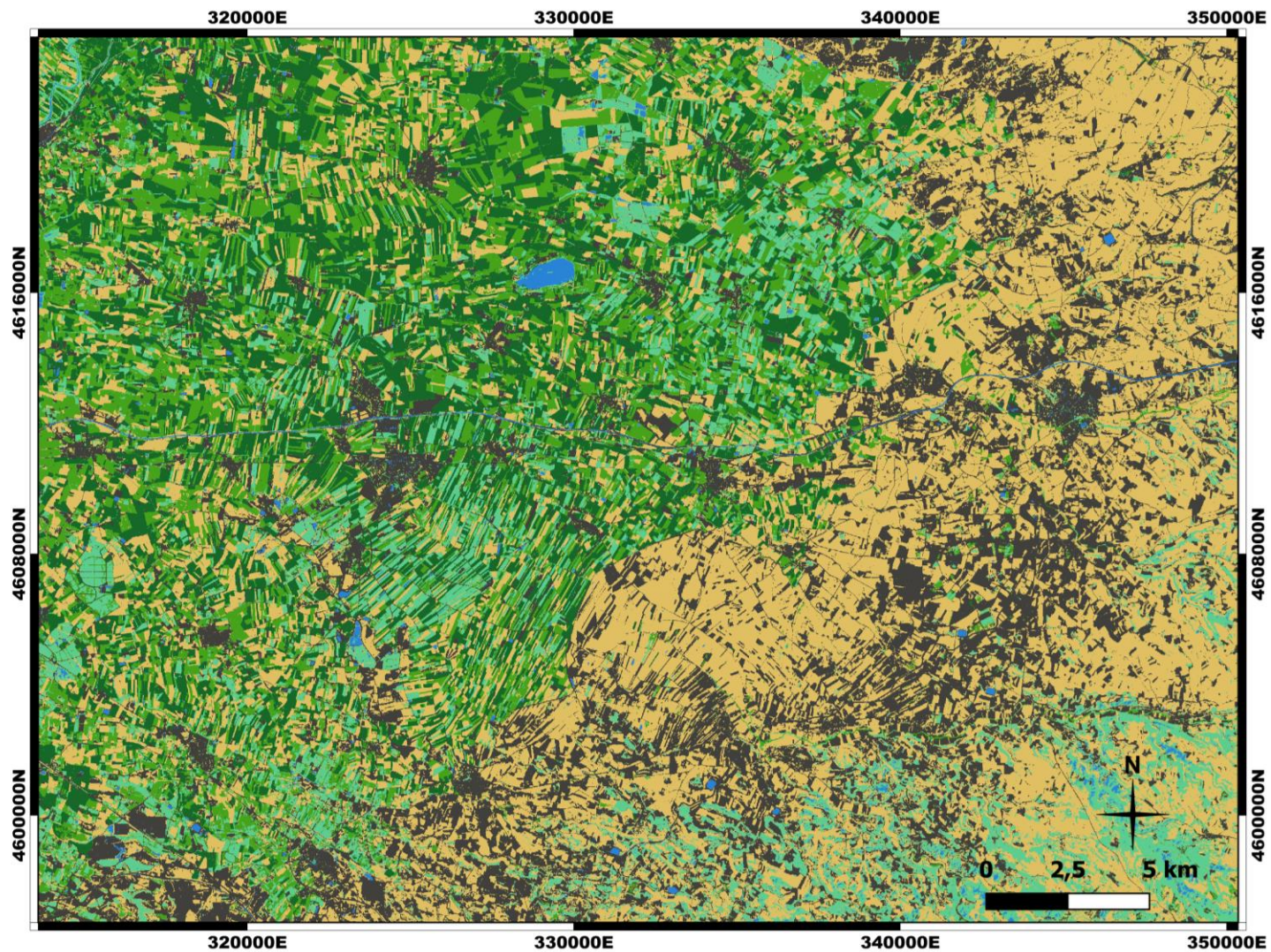
# LIAISE Land use CESBIO v1 dataset







# LIAISE Land use CESBIO v1 dataset



- |  |   |
|--|---|
|  Maize              |  Bare Soil / Dry Grass / Wheat Cut |
|  Alfalfa / Grass    |  Water                             |
|  Pear / Apple trees |  Urban                             |

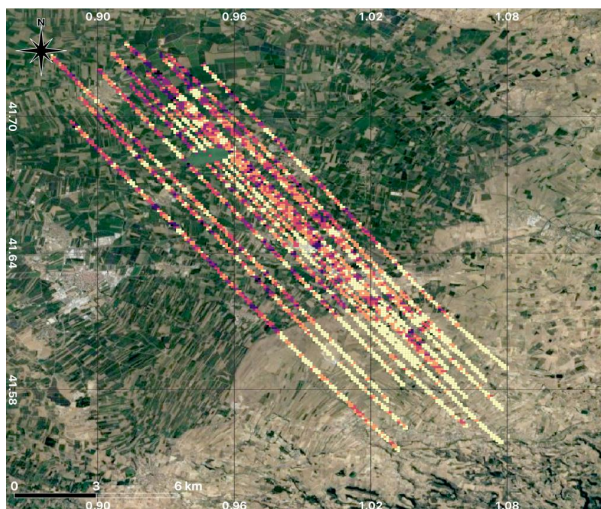


ORFEO ToolBox  
cnes

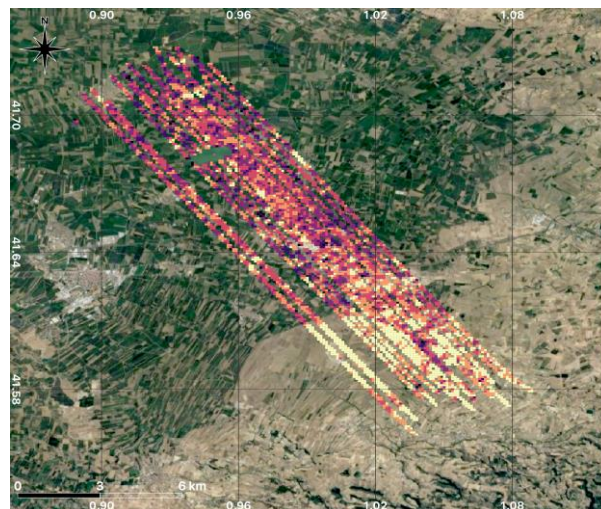
# LIAISE Soil Moisture Estimation CESBIO v1 dataset



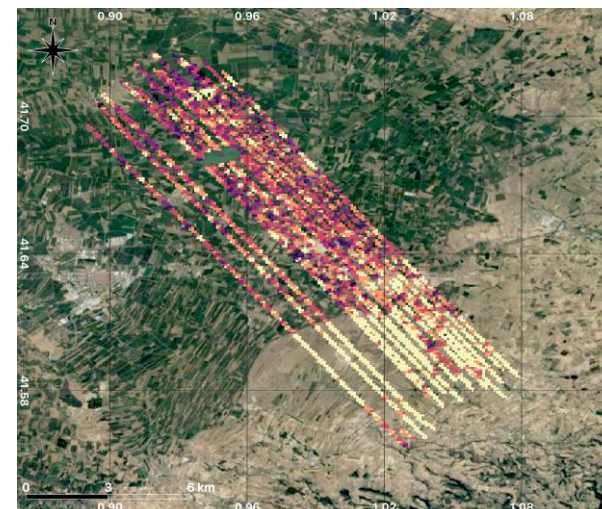
22/07/21 Flight 45 : dry



27/07/21 Flight 46 : wet,  
after a precipitation event



28/07/21 Flight 47 : drying process



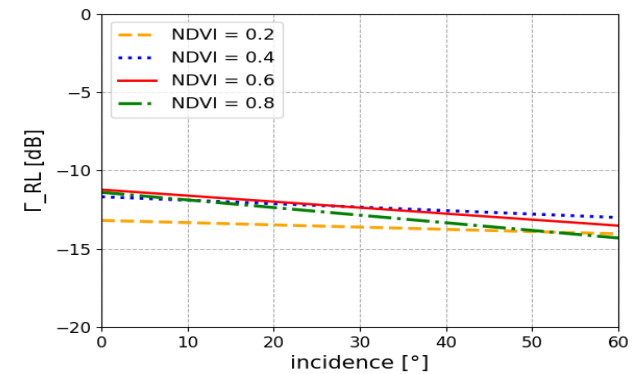
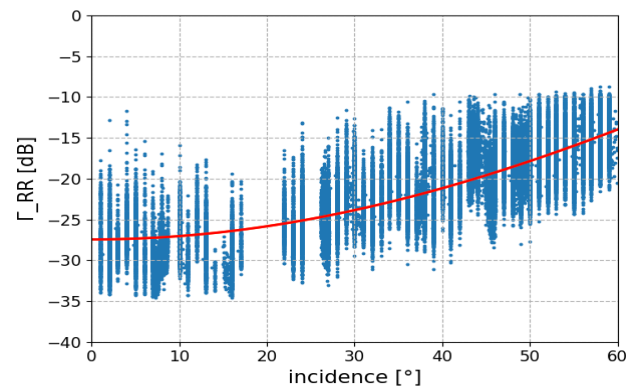
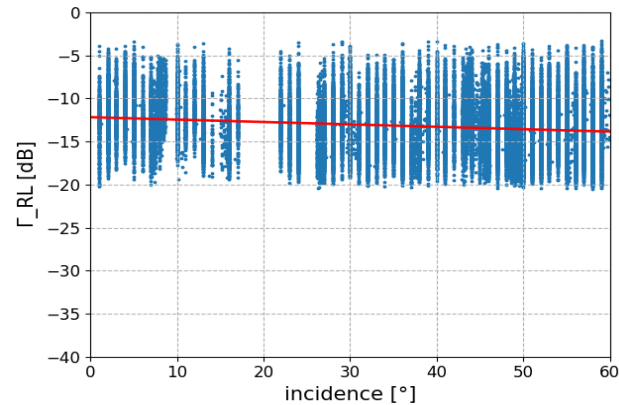
Mv\_est (100m res) [m3/m3]



Inverted maps using a gamma-tau model with reflectivity  $\Gamma_L$

Incidence angle max 40°

# REFLECTIVITY VARIATIONS : FUNCTION OF INCIDENCE ANGLE



$$\Gamma_{RL}(20^\circ) = \Gamma_{RL}(\theta) + b(NDVI)(\theta - 20^\circ)$$

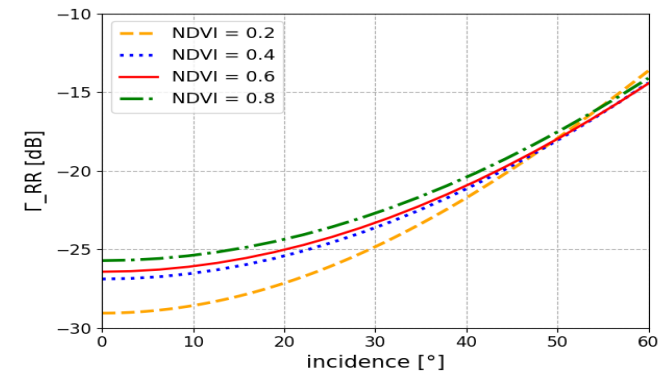
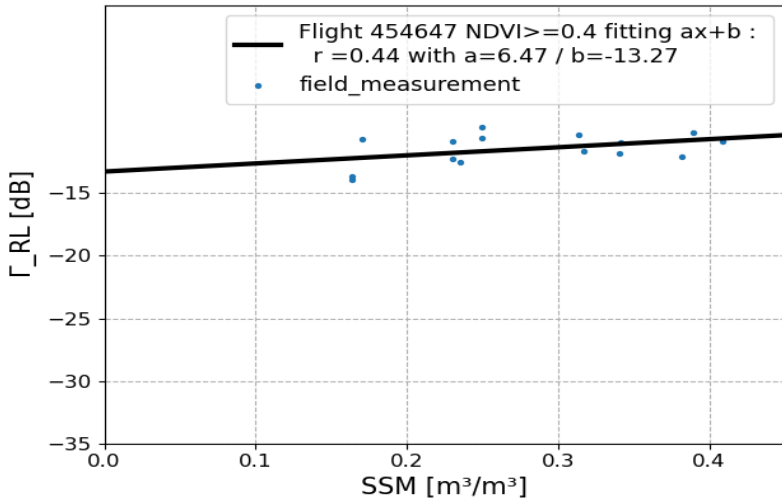
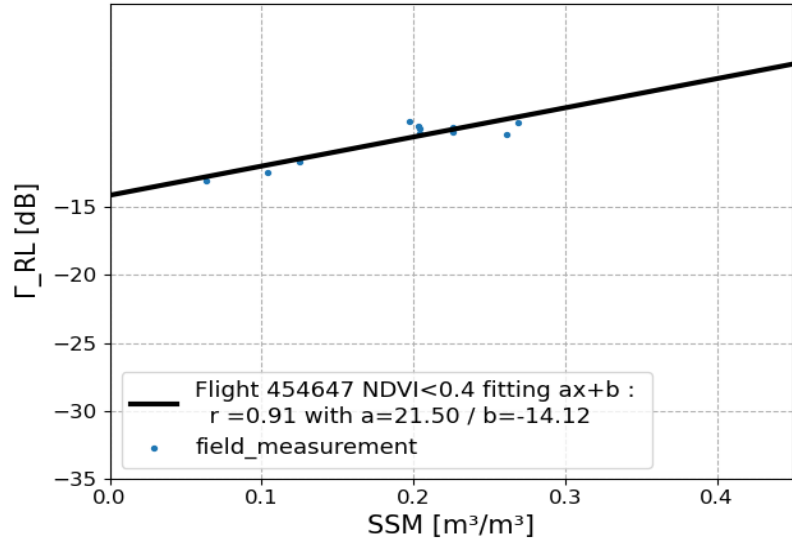


Illustration of GLORI reflectivity data over the Urgell site as a function of incidence angle: a)  $\Gamma_{RL}$  and b)  $\Gamma_{RR}$

$$\Gamma_{RR}(20^\circ) = \Gamma_{RR}(\theta) \left( \frac{\cos(20^\circ)}{\cos(\theta)} \right)^{\beta(NDVI)}$$

R. Fernandez-Moran et al, Remot. Sens. 2017

# REFLECTIVITY SENSITIVITY TO SOIL MOISTURE



$$\Gamma_{pq}(\theta) = \Gamma_{pq}^{soil}(\theta) \cdot e^{-\frac{2\tau_{pq}}{\sin\theta}(1 - \omega_p)^2} \quad \text{V. Zavorotny et al, IEEE 2014}$$

$$\tau_{pq} = c \cdot NDVI$$

$$\Gamma_{pq} = \Gamma_{pq}^{soil} \cdot e^{-2c \cdot NDVI}$$

$$\Gamma_{RL}^{soil} \text{ dB} = \gamma Mv + \delta$$

$$\Gamma_{RL} \text{ dB} = \gamma Mv + \mu NDVI + \delta$$

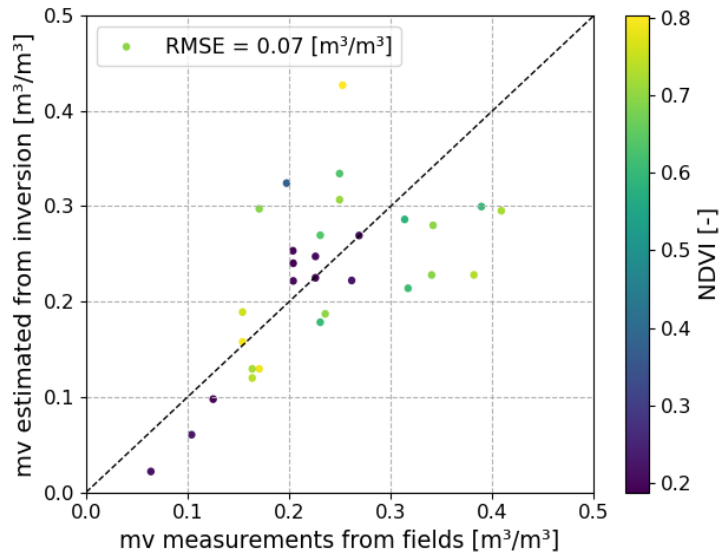
where  $\gamma$  is the sensitivity of the reflectivity to soil moisture,  $\mu$  is the sensitivity of the reflectivity to vegetation growth through the  $NDVI$ , and  $\delta$  is a constant related to the roughness mean effect.

Thus, if we have the  $\Gamma$  reflectivity and the  $NDVI$  level, the soil moisture is estimated using the following equation:

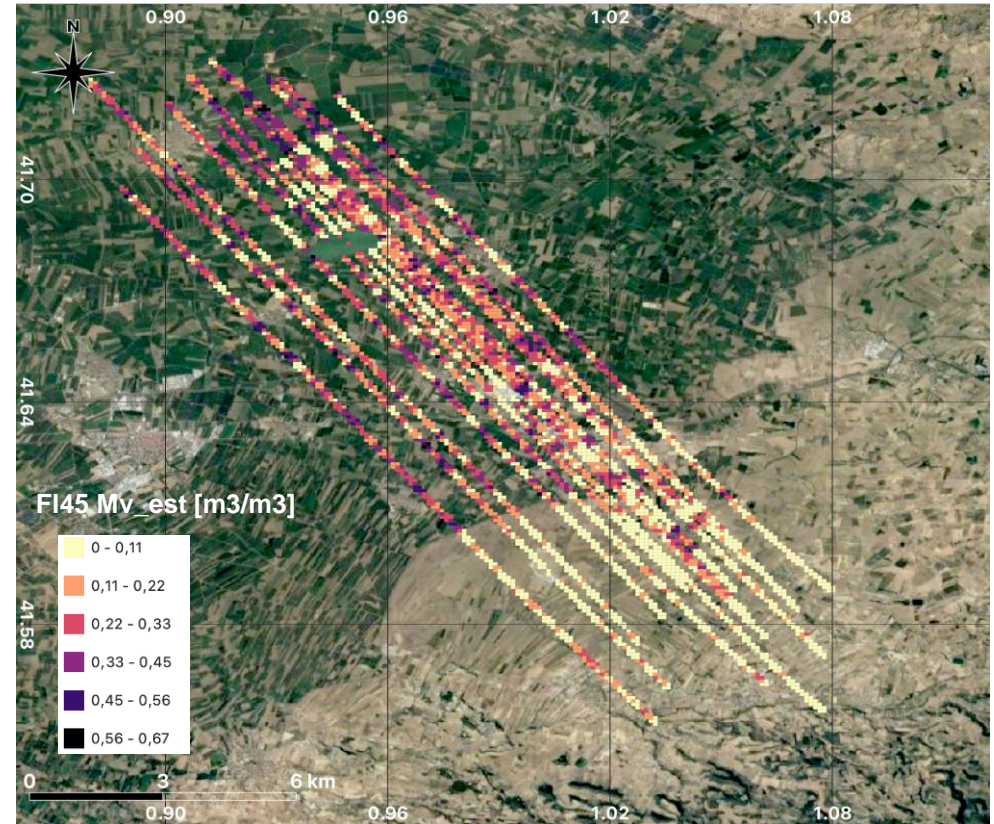
$$Mv = 0.058 \Gamma + 0.28 NDVI + 0.73$$



Calibration of the model with a 3-fold cross-validation approach



Intercomparison between ground measurements and estimated soil moisture from  $\Gamma_{RL}$  data inversion



Map of SSM retrieved from the  $\Gamma_{RL}$  inversion on 22/07/2021, with a spatial resolution equal to 100 m, incidence angle < 40°

$$Mv = 0.058 \Gamma + 0.28NDVI + 0.73$$

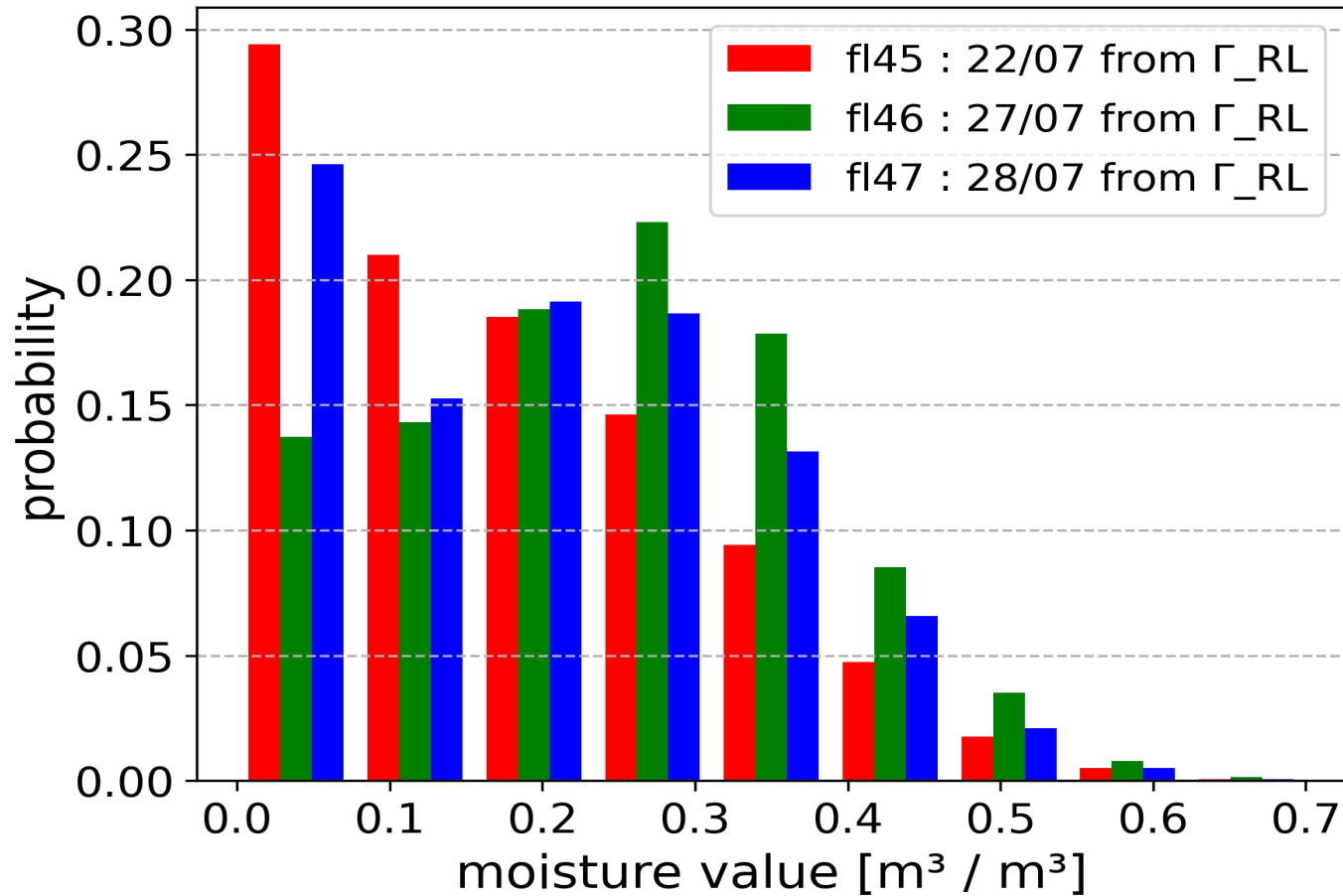


Illustration of soil moisture level distributions over the Urgell site for the three analyzed flights.

**Karin Dassas, Pascal Fanise**, Michel Le Page, Emna Ayari, Philippe Baillion, Mateo Sige, Aaron Boone, **Mehrez Zribi**, Polarimetric instrument Global Navigation Satellite System - Reflectometry airborne data, Data in Brief, Volume 52, 2024, 109850, <https://doi.org/10.1016/j.dib.2023.109850>.

Dataset In situ

Dataset Glori

**Mehrez Zribi**, Vincent Dehaye, **Karin Dassas, Pascal Fanise**, Michel Le Page, Pierre Laluet, Aaron Boone, Airborne GNSS-R polarimetric multi-incidence data analysis for surface soil moisture estimation over an agricultural site, IEEE Journal of Selected Topics in Applied Earth Observations and Remote Sensing, 2022, 10.1109/JSTARS.2022.3208838.

*Warning : dataset Glori in the database has been updated since this paper, same methodology but slight differences in the result*

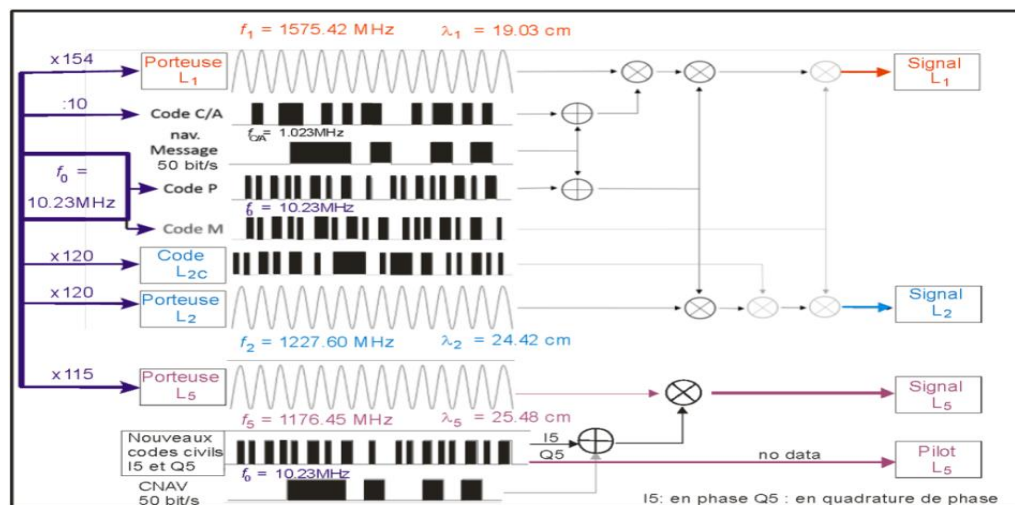
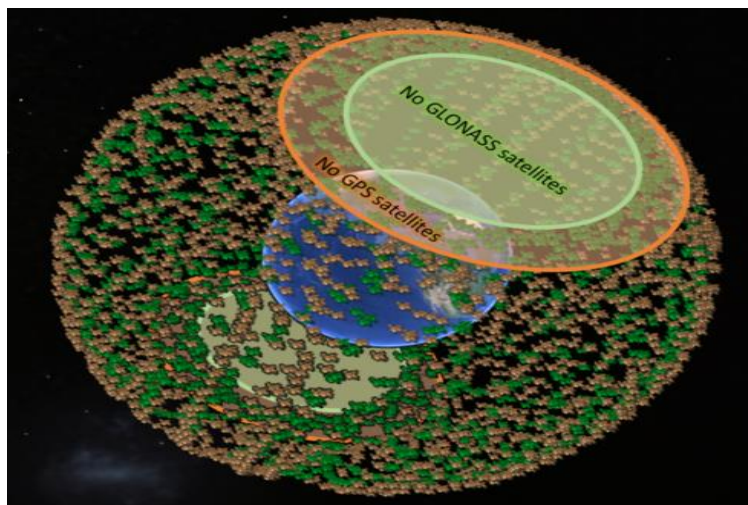
Dataset Land use

Dataset Glori

**M. Zribi, K. Dassas, V. Dehaye, P. Fanise, E. Ayari** and M. Le Page, "Analysis of Polarimetric GNSS-R Airborne Data as a Function of Land Use," in *IEEE Geoscience and Remote Sensing Letters*, vol. 20, pp. 1-5, 2023, Art no. 2502105, doi: 10.1109/LGRS.2023.3270730.

**Thanks for your attention!**

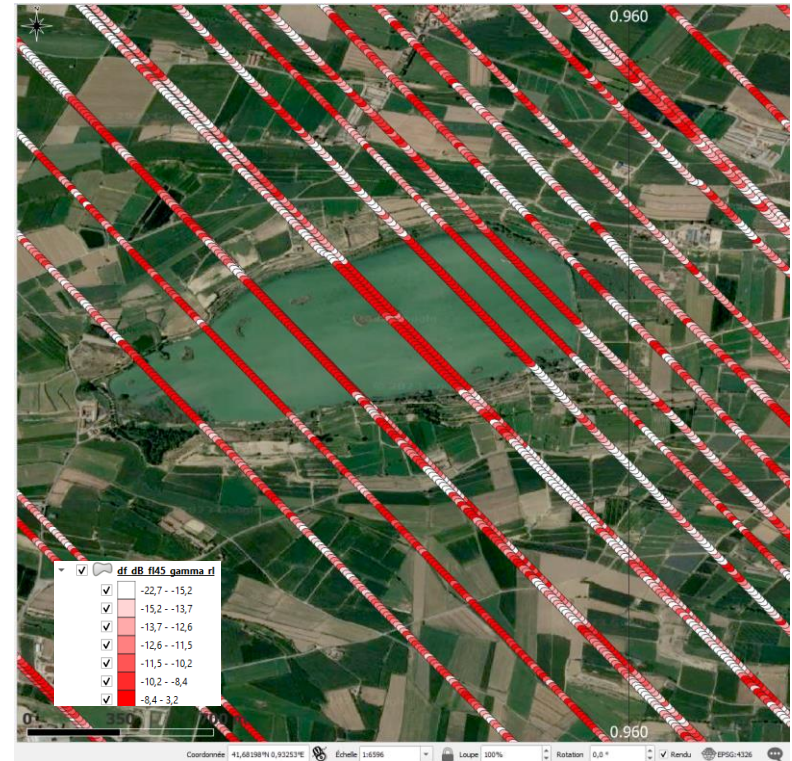
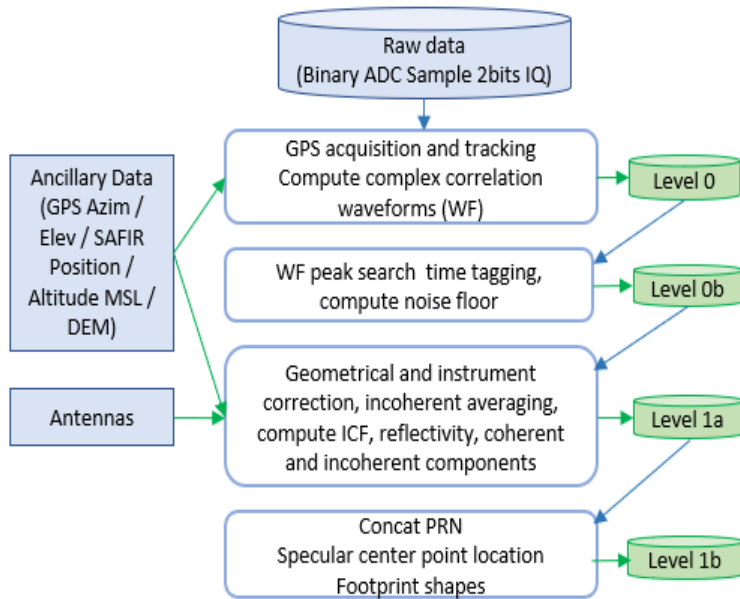
# Backup



Here we can see the dense coverage of the two oldest GNSS constellations: the American GPS (orange) and the Russian system GLONASS (green).

Structure of the GPS signal (L1 for Glori, soon L5)





$$\text{Cross-correlated waveform : } Y(\tau, f) = \frac{1}{T_i} \int_{T_i} u_{d,r} a(t - \tau) e^{i(f_c + f)t} dt$$

Corrected ICF = Interferometric Complex Field

$$ICF_{corr} = \frac{|Y_{r,max}| - B_r}{|Y_{d,max}| - B_d} e^{j(\phi_{r,max} - \phi_{d,max})} \frac{G_d}{G_r}$$

$$\Gamma'_{pq} = \left| \left\langle \frac{Y_{r,q}(\Delta\tau, f)}{Y_{d,p}(0, f)} \right\rangle \right|^2$$

$$\Gamma'_{pq} = \left\langle |ICF_{corr,pq}|^2 \right\rangle - \sigma_{|ICF_{corr,pq}|}^2$$

E. Motte et al, sensors, 2016  
A. Egido et al, IEEE 2014



# NORMALIZED GLORI DATA MAPPING

